Observation of Single-Mode Operation in a Free-Electron Laser

Luis R. Elias, Gerald Ramian, James Hu, and Avner Amir

Physics Department and Quantum Institute, University of California, Santa Barbara, Santa Barbara, California 93106

(Received 2 December 1985)

Time-structure and frequency-spectrum measurements of our free-electron-laser oscillator show that for periods shorter than 5 μs the laser operates in a stable single-cavity mode having a strikingly small fractional frequency bandwidth of 10^{-8}. This constitutes the first demonstration of high-temporal-coherence operation of a free-electron laser. For periods longer than 5 μs the laser frequency changes in unexpected quantized steps which may be explained in terms of a homogeneously broadened gain profile coupled to a small monotonic drift in electron-beam energy.

PACS numbers: 42.55.Tb

Together with high power, high efficiency, and continuous frequency tunability, free-electron lasers (FEL's) have the potential capability of operating with a very high degree of temporal coherence. However, this last feature has not been and will not be observed in FEL oscillator experiments driven by short-electron-pulse accelerators, as is the case with the three rf-accelerator FEL oscillator experiments carried out at Stanford University,[1] Los Alamos National Laboratory (LASL),[2] and Orsay, France.[3] In all of these experiments short electron pulses, ranging in length from a few picoseconds up to a few nanoseconds, were injected periodically into the FEL interaction region forcing the resonator radiation field to bunch into short broad-band optical pulses involving the phase locking of many longitudinal cavity modes. Table I summarizes the frequency structure of reported FEL oscillator experiments. In contrast, the University of California, Santa Barbara (UCSB), FEL employs an electrostatic accelerator which is presently capable of generating variable-length electron pulses from 1 to 50 μs. In this Letter, we report the first operation of a single-mode FEL oscillator. We also present data showing that the oscillating mode is quite stable against sudden changes in the resonance parameter, such as small shifts in beam energy. We also report that the sideband instability predicted by Kroll and Rosenbluth[4] and first reported by the Los Alamos group has not been observed in the UCSB FEL.

A description of the UCSB FEL experimental hardware has been discussed elsewhere.[5] A schematic drawing of the resonator is shown in Fig. 1. It is constructed from two horizontal, parallel, stainless-steel plates having two cylindrical copper mirrors located between them in a nearly confocal arrangement. The cold modes of this type of resonator, as well as their excitation by spontaneous emission, have been analyzed in detail elsewhere.[6] These consist of linearly polarized cylindrical waves having a Hermite-Gaussian amplitude modulation in one direction, with the electric field parallel to the metal plates, and a cosine amplitude modulation in the other transverse direction.

The mathematical representation of the traveling modes is

$$\Psi_{m,n}=\left[\frac{1}{\pi^{1/2}\omega(z)}\right]^{1/2}\exp\left\{-\frac{x^2}{2w^2}+i\left[\frac{\alpha_n x^2}{2R}+\alpha_n z-kct-(m+\tfrac{1}{2})\tan^{-1}\left(\frac{z}{z_r}\right)\right]\right\}\cos\left(\frac{n\pi y}{b}\right)H_m\left(\frac{x}{w}\right),$$

$$\alpha_n=\left[k^2-\left(\frac{n\pi}{b}\right)^2\right]^{1/2}, \quad (1)$$

where $w(z)$, z_r, and $R(z)$ are respectively the wave's Gaussian beam radius, Rayleigh length, and radius of curvature. The index n and the propagation constant α_n are associated with the guided portion of the wave, while the index m is the order of its Hermite-Gaussian modulation. The separation between the plates is b and the angular

TABLE I. Spectral characteristics of reported FEL oscillator experiments.

Group	Wavelength (μm)	Fractional bandwidth	Number of modes
Stanford	3.4	2×10^{-3}	16 000
LASL	10.6	3×10^{-3}	4 600
Orsay	0.517	6×10^{-4}	13 000
UCSB	150	1.6×10^{-8}	1

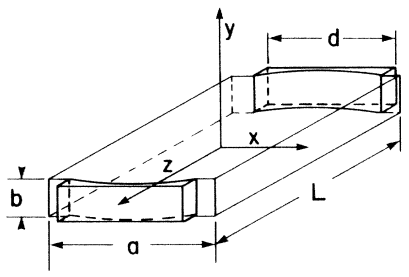

FIG. 1. Schematic drawing of the UCSB FEL resonator.

frequency of the wave is kc. The cold-resonator frequencies are

$$\omega_{m,n,q} = (c/L)\{[\pi q + 2(m+\tfrac{1}{2})\tan^{-1}(L/2z_r)]^2 + (n\pi L/b)^2\}^{1/2}, \quad (2)$$

where q is the axial mode index and L is the resonator length.

Although all cold-cavity modes can accept radiation, the FEL mechanism allows radiation only into those modes satisfying the modified FEL synchronism condition

$$(d/dz)[(k_0+\alpha_n)z - kct - (m+\tfrac{1}{2})\tan^{-1}(z/z_r)] = 0. \quad (3)$$

At the beam waist, the resulting quadratic equation in k yields the following possible traveling-wave frequencies:

$$\nu_{n,m} = (c\gamma_z^2\beta_z\epsilon_m/\lambda_0)\{1 \pm \beta_z[1-(n\lambda_0/2b\gamma_z\beta_z\epsilon_m)^2]^{1/2}\}, \quad \epsilon_m = 1-(m+\tfrac{1}{2})/k_0 z_r, \quad (4)$$

where β_z is the average normalized axial velocity of the electron and $\gamma_z = (1-\beta_z^2)^{-1/2}$.

In addition to transverse modes, the cavity supports longitudinal modes spaced by $c/2L$, where L is the length of the resonator. Table II summarizes the frequency differences between adjacent cavity modes when the various indices are changed by one unit.

The first laser time-structure measurements were carried out with a modestly fast InSb Putley detector.[7] Oscilloscope traces (Fig. 2) describe the temporal response of the laser to both a short [Fig. 2(a)] and a long [Fig. 2(b)] electron-beam pulse. For the long electron pulse a series of unexpected laser power fluctuations were observed to occur every 5 μs. It was initially thought that these power fluctuations were associated with the consecutive excitation of adjacent transverse resonator modes. However, that explanation was discarded because the measured laser frequency difference of 3.7 GHz between consecutive temporal laser peaks was smaller than any of the calculated frequency differences between the transverse modes listed in Table II. Further confirmation of the single-transverse-mode operation came about when the same laser power fluctuations were observed after insertion of a spatial mode filter into the cavity.

The bandwidth of the laser, averaged over may electron pulses, was obtained by use of a far-infrared Fabry-Perot (FP) interferometer and a gated integrator as shown in Fig. 3. Figure 4 illustrates a typical low-resolution (i.e., first order) interferogram obtained with the gated integrator set to sample the first [Fig. 4(a)], the second [Fig. 4(b)], and the first plus the second [Fig. 4(c)] optical power peaks shown in Fig. 5.

TABLE II. Frequency difference between resonator modes.

Fundamental-mode frequency	$\nu_{0,1,q} = 2.0$ THZ
Transverse-mode frequency spacing	$\nu_{0,1,q} - \nu_{0,3,q} = 30.5$ GHZ
	$\nu_{0,1,q} - \nu_{2,1,q} = 8.0$ GHZ
Longitudinal-mode frequency spacing	$\nu_{0,1,q} - \nu_{0,3,q+1} = 20.0$ MHz
Gain bandwidth	$\nu_{0,1,q}/2N^{a} = 6.0$ GHZ

[a] N is the number of undulator periods.

The bandwidths of the scans shown in Fig. 4 are due to the low resolution of the FP interferometer. The measurements shown in Fig. 4 were repeated after an increase in the resolution of the FP interferometer from 10% (first order) to 0.06% (120th order) at 240 μm.

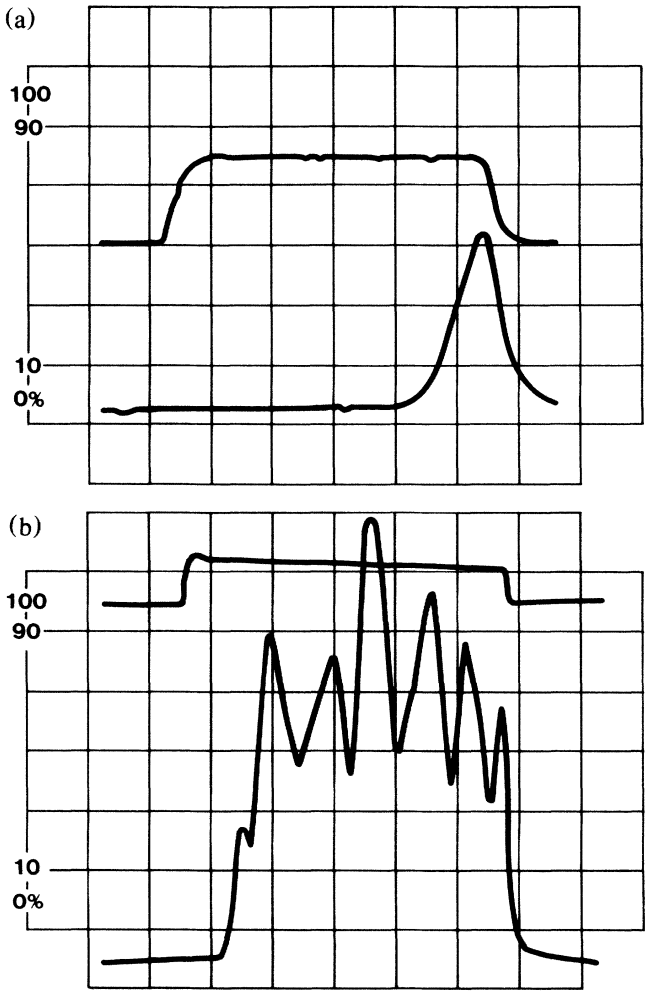

FIG. 2. Time structure of the FEL power output (lower trace) and electron-beam current (upper trace) for (a) a short electron pulse (1 μs/div) and (b) a long electron pulse (6.25 μs/div).

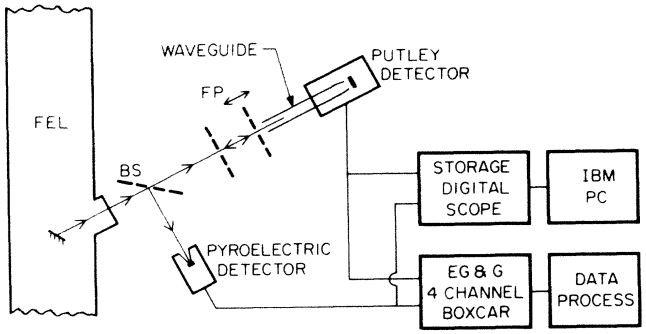

FIG. 3. Signal-detection setup for measurement of the time-averaged frequency spectrum of the laser and its single pulse time structure.

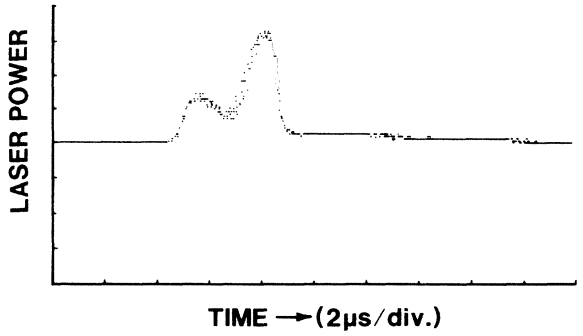

FIG. 5. Time structure of a double laser pulse obtained with a very fast Schottky diode detector.

From the high-resolution traces shown in Fig. 6 two very important results should be noted: First, the spectrum of the laser averaged over many electron pulses yields a fractional bandwidth close to 0.1%; and second, there are strong fluctuations in the amplitude of the signal transmitted by the FP interferometer while no such signal fluctuations were observed in the reference detector, indicating strong modulation by the FP bandpass slopes. The combination of these two results demonstrates that during each laser pulse the frequency bandwidth of the FEL is much narrower than the transmission bandwidth (0.06%) of the FP interferometer. However, the center frequency of each laser pulse fluctuates by 0.1% because of very small ($\simeq 0.05\%$) electron energy fluctuations existing from pulse to pulse. In conclusion, what was measured with the FP interferometer was the very narrow bandwidth of the laser pulses broadened by the pulse-to-pulse frequency fluctuations resulting from electron-energy instabilities.

Finally, the frequency spectrum of a single pulse was derived from the Fourier transform of the temporal structure [Fig. 7(a)] measured with a Schottky-diode detection system having a 1-ns response time. If the laser signal consisted of a single longitudinal mode, the Schottky-diode square-law detector would have generated a signal characterized by an unmodulated pulse. However, if more than one longitudinal mode had been excited with comparable amplitude, the pulse would have shown an additional strong modulation at the sum and difference frequencies of the longitudinal oscillating modes. No such strong signal modulation is present, as shown in Fig. 7(a); instead, it is possible to observe only a small amount of high-frequency noise riding over the pulse. From an amplified view of the noise portion of the signal shown in Fig. 7(b), it can be seen that the noise is actually a small coherent signal at 20.1- and 40.2-MHz frequency, corresponding to the weak excitation of two additional longitudinal modes. The final conclusion is that the laser is oscillating in a single-cavity mode with a bandwidth narrower than the separation between longitudinal modes. An estimated laser bandwidth of 30 kHz was obtained from the Fourier transform of the laser amplitude modulation shown in Fig. 7(a). This corresponds to a fractional signal-pulse laser bandwidth of 1.6×10^{-8}.

The laser-power time structure shown in Fig. 2(b) can be explained in terms of the excitation of a single

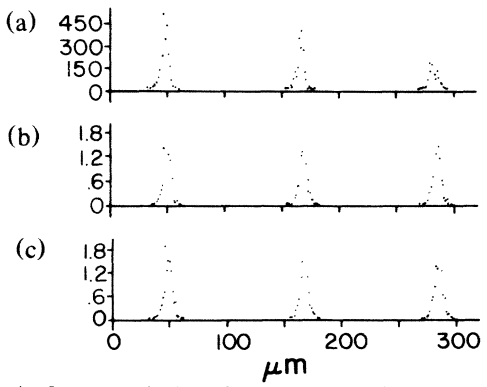

FIG. 4. Low-resolution time-averaged Fabry-Perot interferogram of (a) the first, (b) the second, and (c) the first plus the second laser pulse shown in Fig. 5.

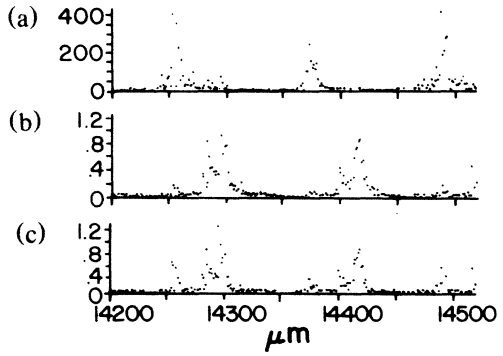

FIG. 6. Same as Fig. 4, but after increase of the FP instrument resolution from 10% to 0.6%. Large amplitude fluctuations, as well as the 3.5-GHz frequency difference between peaks, is apparent.

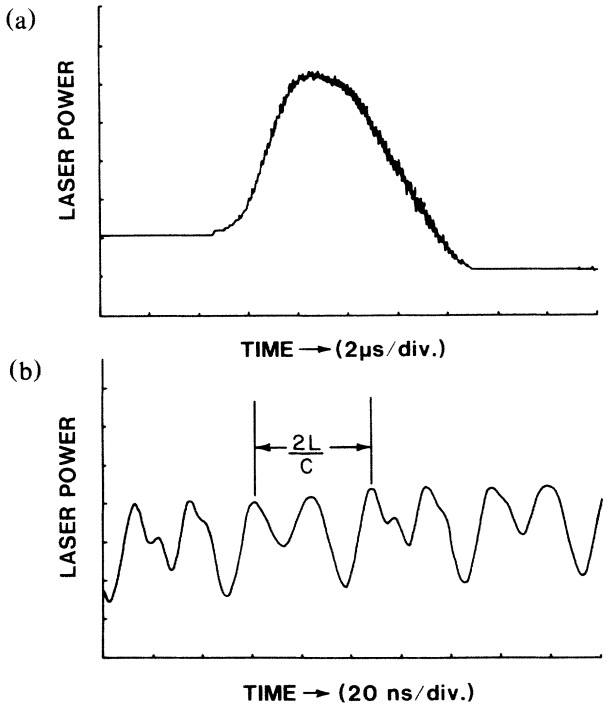

FIG. 7. (a) Time structure of a single laser pulse obtained with a fast Schottky diode detector and (b) amplified time structure of the top of the pulse showing the low-amplitude beat oscillation of two longitudinal modes. Estimated peak power is about 10 kW. The frequency difference between the two modes is 20 MHz.

cavity mode and the small monotonic drift of electron energy toward lower values. The voltage of the UCSB electrostatic accelerator drifts at a rate $\dot{V} = \dot{V}_0(1-R)$, where R is the beam recovery efficiency and $\dot{V}_0 = I/C$ is the rate of voltage change with no beam recovery. I and C are respectively beam current and accelerator terminal capacitance.[7] The monotonic decrease in beam voltage gives rise to a continuous rate of change in FEL resonance frequency of $\dot{\nu}_r/\nu_r \simeq 2\dot{V}/V$. With a beam recovery of 90%, a beam current of 1.25 A, a 150-pF capacitance, and a resonance frequency of 2 THz, $\dot{\nu}_r$ is approximately 0.7 GHz/μs. In 5 μs the total shift in frequency of 3.5 GHz compares well with the measured value of 3.7 GHz. What is important to recognize here is that although the resonance frequency of the laser is changing continuously with time, the actual laser frequency changes occur in quantized steps of 3.7 GHz every 5 μs.[8] With greater beam recovery or implementation of a terminal voltage stabilizer, it will be possible to operate the UCSB FEL in a single cavity mode over a period of time much longer than 5 μs and, consequently, even narrower bandwidth.

The question of the fundamental FEL linewidth under ideal conditions (i.e., in the absence of the energy drift) has also been investigated theoretically and will be published elsewhere.[9]

The authors wish to thank B. J. Clifton from Lincoln Laboratory and N. Luhman from the University of California, Los Angeles, for providing us with Schottky-diode receivers.

[1]L. R. Elias *et al.*, Phys. Rev. **36**, 717 (1976); D. A. G. Deacon *et al.*, Phys. Rev. Lett. **38**, 897 (1977).

[2]B. E. Newman *et al.*, Nucl. Instrum. Methods Phys. Res., Sec. A **237**, 187 (1985).

[3]P. Elleaume, Nucl. Instrum Methods Phys. Res., Sect. A **237**, 38 (1985); M. Billardon *et al.*, Nucl. Instrum. Methods Phys. Res., Sect. A **238**, 244 (1985).

[4]N. M. Kroll and M. N. Rosenbluth, in *Free-Electron Generators of Coherent Radiation,* edited by S. F. Jacobs, H. S. Pilloff, M. Sargent, III, M. O. Scully, and R. Spitzer, Physics of Quantum Electronics Vol. 7 (Addison-Wesley, Reading, MA, 1980), Chap. 6, p. 147.

[5]L. R. Elias and G. J. Ramian, in *Free-Electron Generators of Coherent Radiation,* edited by C. Braw, S. Jacobs, and M. O. Scully (SPIE, Bellingham, Washington, 1984), Vol. 453, p. 137.

[6]L. R. Elias and J. C. Gallardo, Appl. Phys. B **31**, 229 (1983); A. Amir *et al.*, Phys. Rev. A **32**, 2864 (1985).

[7]E. H. Putley, Appl. Opt. **4**, 649 (1965).

[8]A. Amir *et al.*, Appl. Phys. Lett. **47**, 1251 (1985).

[9]A. Gover, A. Amir, and L. R. Elias, to be published.